PROCEEDINGS B

rspb.royalsocietypublishing.org

Research

Cite this article: Cheng BS, Chang AL, Deck A, Ferner MC. 2016 Atmospheric rivers and the mass mortality of wild oysters: insight into an extreme future? *Proc. R. Soc. B* **283**: 20161462.
http://dx.doi.org/10.1098/rspb.2016.1462

Received: 8 July 2016
Accepted: 31 October 2016

Subject Areas:
ecology, environmental science, physiology

Keywords:
atmospheric river, climate change, extreme, flood, mass mortality event, oyster

Author for correspondence:
Brian S. Cheng
e-mail: bscheng@gmail.com

Electronic supplementary material is available online at https://dx.doi.org/10.6084/m9.figshare.c.3575207.

THE ROYAL SOCIETY PUBLISHING

Atmospheric rivers and the mass mortality of wild oysters: insight into an extreme future?

Brian S. Cheng[1,2], Andrew L. Chang[3,4], Anna Deck[3] and Matthew C. Ferner[3]

[1]Bodega Marine Laboratory, University of California, Davis, Bodega Bay, CA 94923, USA
[2]Smithsonian MarineGEO, Smithsonian Environmental Research Center, Edgewater, MD 21037, USA
[3]San Francisco Bay National Estuarine Research Reserve, San Francisco State University, Tiburon, CA 94920, USA
[4]Smithsonian Environmental Research Center, Tiburon, CA 94920, USA

BSC, 0000-0003-1679-8398

Climate change is predicted to increase the frequency and severity of extreme events. However, the biological consequences of extremes remain poorly resolved owing to their unpredictable nature and difficulty in quantifying their mechanisms and impacts. One key feature delivering precipitation extremes is an atmospheric river (AR), a long and narrow filament of enhanced water vapour transport. Despite recent attention, the biological impacts of ARs remain undocumented. Here, we use biological data coupled with remotely sensed and *in situ* environmental data to describe the role of ARs in the near 100% mass mortality of wild oysters in northern San Francisco Bay. In March 2011, a series of ARs made landfall within California, contributing an estimated 69.3% of the precipitation within the watershed and driving an extreme freshwater discharge into San Francisco Bay. This discharge caused sustained low salinities (less than 6.3) that almost perfectly matched the known oyster critical salinity tolerance and was coincident with a mass mortality of one of the most abundant populations throughout this species' range. This is a concern, because wild oysters remain a fraction of their historical abundance and have yet to recover. This study highlights a novel mechanism by which precipitation extremes may affect natural systems and the persistence of sensitive species in the face of environmental change.

1. Introduction

There is growing concern for the increased prevalence and intensity of extreme events under climate change [1,2]. Extremes such as heatwaves, drought, and intense precipitation are more common under a warming climate. For example, the European heatwave of summer 2003 was the hottest since year 1500 [3], and anthropogenic climate change appears to have at least doubled the risk of an extreme event of that magnitude [4]. In the USA, extreme precipitation events have increased in frequency by approximately 33% over the last 100 years [5] and in California, multi-model simulations suggest that by year 2100, both intense drought and flooding may increase in frequency by at least 50% [6]. Warming is expected to intensify these extremes partly because of the physical effects of warming on atmospheric conditions. The warming of air results in an exponential increase in atmospheric water-holding capacity (Clausius–Clapeyron equation; +1°C increases the moisture capacity of saturated air by 7%), which can facilitate extreme precipitation and provide greater latent energy to drive storms [7]. Despite mounting evidence for the ongoing intensification of these extremes, the ecological consequences of such events remain unclear, in part, due to the rarity of ecological data before and after these unpredictable events [8]. Although heatwaves and thermal stress have provided some insights into the biological consequences of extremes (e.g. mass mortality, complex range shifts, community reorganization; [9–11]), our understanding of the

impacts of extreme precipitation events and their linkage to climate change remain poorly resolved.

Recent work has revealed a critical role for atmospheric rivers (ARs) in driving extreme precipitation events [12–16]. An AR is a long and narrow corridor of enhanced water vapour that traverses the lower atmosphere. ARs are responsible for more than 90% of the mid-latitude poleward moisture flux on the Earth and are thus a critical component of the global water cycle [15,16]. ARs and their associated precipitation are global features that have been detected across all continents [17,18]. In California, ARs deliver up to one-half of the state's entire annual precipitation over the course of only 10–15 days [19]. ARs have been linked to all seven declared floods from 1996 to 2007 on California's Russian River [13] and in Britain, all 10 of the largest floods since the 1970s were associated with ARs [20]. Climate change is projected to increase the intensity and frequency of ARs, as well as prolong the AR season [21,22]. Despite this currently recognized importance of ARs in driving extreme floods and influencing global water cycles, to the best of our knowledge, no study has documented their biological impacts.

A potential consequence of extreme or transient events is the mass mortality of wild populations. Mass mortality events (MMEs) are infrequent and substantial declines in population size that occur on abrupt timescales. The likelihood of an MME is related to both the generation time of the affected species and the frequency and magnitude of disturbance [23]. Species that undergo MMEs may require decades to recover, and in extreme cases, MMEs may trigger extinction vortices via environmental stochasticity or Allee effects [24,25]. If MMEs affect foundation species, then cascading effects throughout the biological community may also arise. For example, the 1983–1984 mass mortality of the herbivorous urchin *Diadema antillarum* throughout the Caribbean has been linked to a subsequent phase shift from coral- to algal-dominated tropical reef communities [26]. Moreover, the severity of MMEs among avian, fish, and marine invertebrate taxa appears to be increasing [27], highlighting the need to clarify their causes and patterns of occurrence.

MMEs may be a significant hurdle to the conservation and restoration of coastal marine organisms such as oysters, which are foundation species that provide numerous ecosystem functions (e.g. filtration, habitat creation, benthic–pelagic coupling; [28,29]). Over the last century, wild populations of native oysters in the USA, Olympia oysters (*Ostrea lurida*) on the western coast, and eastern oysters (*Crassostrea virginica*) on the eastern and southern coasts, have undergone an 88% decline in biomass and a 64% decline in oyster bed areal extent [30]. This decline was largely driven by overfishing and habitat degradation [31,32]. On the west coast of the USA, the Olympia oyster is the focus of restoration efforts, but populations remain a fraction of what they once were. One of the most abundant populations of Olympia oysters resides in northern San Francisco Bay, California (CA), USA, where at times, densities may be an order of magnitude greater than elsewhere within San Francisco Bay and in other estuaries (electronic supplementary material, appendix S1; [33,34]). Here, we integrate remotely sensed, environmental time series, and field observational data to describe the contribution of ARs to an extreme low salinity event and the consequent near 100% mass mortality of wild Olympia oysters within northern San Francisco Bay. This study provides the first evidence for the biological consequences of ARs and highlights a new mechanism underlying precipitation extremes and their subsequent ecological impacts.

2. Methods

(a) Study system

We combined remotely sensed and environmental time-series data with biological sampling to describe drivers of oyster abundance and survival in northern San Francisco Bay (electronic supplementary material, appendix S2). We focused on China Camp State Park in Marin County, CA, because this location has a robust water quality sampling programme, and this region may be prone to extreme low salinity events because of its position within the estuary. San Francisco Bay drains a vast watershed, an area encompassing approximately 40% of California, resulting in substantial freshwater input through the Sacramento–San Joaquin River Delta (hereafter 'delta'; [35]). Heightened freshwater flows from the delta into northern San Francisco Bay can result in protracted low salinity events. These events are highly seasonal, because a Mediterranean climate regime results in dry summer and autumn seasons, whereas precipitation is largely concentrated in the winter, followed by snowmelt discharge in the spring [35]. Both downscaled and global climate models for this region project high interannual variability with future years of intense flooding as well as years of drought [6,36,37].

(b) Physical drivers

A key physical driver of the dynamics within estuaries is the input of freshwater. To quantify freshwater influx into San Francisco Bay, we used results from a widely applied model ('Dayflow'; see 'Data accessibility' for data sources) that produces a daily average estimate of delta freshwater flow at Chipps Island, CA (electronic supplementary material, appendix S2). Noting the presence of an extreme freshwater discharge event in late March 2011, we examined a database of AR occurrence, focusing on water year 2011 (1 October 2010–30 September 2011). This database uses remotely sensed water vapour imagery to identify ARs, defined as long (more than 2 000 km) and narrow (less than 1 000 km) corridors of enhanced water vapour content (more than 2 g cm^{-2}; [13,16,38]). Water vapour data are produced by special sensor microwave imager/sounders orbiting the Earth onboard Defense Meteorological Satellite Programme satellites. From this database, we extracted the occurrence of landfalling ARs that intersected the California coast [32.5–41.0°N] and were present in either: the morning or afternoon satellite pass on any given day (hereafter 'AR1s') or present in both satellite passes (hereafter 'AR2s'; [39]) prior to the extreme discharge event. To describe patterns of precipitation associated with ARs, we extracted data from 19 precipitation stations (electronic supplementary material, appendix S3) located throughout the Sierra Nevada Mountain Range that comprise three indices located within the San Francisco Bay watershed. We chose these stations because the combination of high water vapour content (from ARs) directed towards elevated terrain promotes heavy orographic precipitation (i.e. condensation of moisture-laden air that results in rain or snow). Each index represents the northern, central, and southern portions of the Sierra Nevada Mountain Range (i.e. 'Northern Sierra 8', 'San Joaquin 5', and the 'Southern Sierra 6'). For this time frame, we excluded two stations because of missing data (appendix S3). We classified precipitation as 'AR associated' if it fell on the same day as AR landfall plus one lag day. We chose this approach because it ameliorates event splitting

(i.e. when an AR begins on one day and ends on the next) and because this is an appropriate duration when considering the relationship between precipitation and subsequent river discharge [40]. Finally, this approach is consistent with other studies examining ARs and their hydrological effects in western USA [19,40]. Precipitation falling on any other day was classified as 'non-AR'. To place water year 2011 into a broader context of precipitation, we accessed a multi-decadal (93–102 years) dataset of cumulative monthly precipitation for the same indices described above (using all 19 stations).

To examine the local effects of precipitation on salinity and other environmental conditions (i.e. temperature, pH_{NBS}, dissolved oxygen), we used National Estuarine Research Reserve System (NERRS) long-term monitoring data. We accessed data from 2009 to 2014 (coinciding with biological sampling described below) collected by a multi-parameter sonde (6600 series, YSI Incorporated, OH, USA) positioned 0.25 m above the seafloor (1.2 m average depth) at China Camp State Park (electronic supplementary material, appendix S2). *In situ* water quality measurements taken during regular site visits indicate that the sonde data are representative of conditions experienced at the monitoring sites described below (BS Cheng 2016, unpublished data). The sonde logged data every 15 min and was calibrated monthly and data was passed through NERRS quality assurance and control. Because tidal flows can influence the salinity regime and alter the duration of low salinity events [41], we also extracted observed sea-level data from a nearby tide gauge (National Oceanic and Atmospheric Administration Station 9414863).

In order to relate the environmental time-series data to oyster demography, we collated oyster physiological tolerance and performance data from the published literature. This information describes the environmental conditions over which oysters are able to persist in response to: water/air temperature, salinity, dissolved oxygen, and pH (electronic supplementary material, appendix S4). In particular, we extracted an estimate of minimum salinity tolerance (S_{crit}) from Cheng *et al.* [42], who subjected San Francisco Bay oysters to low salinity treatments of varying magnitudes (salinities = 5, 10, 15, 33) and duration (1–8 days).

(c) Biological monitoring

We integrated physical data with biological monitoring data from three sources. First, we monitored three field sites within China Camp (electronic supplementary material, appendix S2; Rat Rock, Village North, and Weber Point), which are located within 0.3–1.0 km of the water quality sonde described above. We visited each site every three months from October 2009 to July 2011. We used a hierarchical sampling protocol because of extremely high oyster densities at the beginning of the census. For each site and time point, we randomly selected nine 0.25 m^2 quadrats in the intertidal zone (three quadrats each at 0.0, 0.05, and 0.1 m mean lower low water, MLLW). Within each quadrat, we quantified oyster abundance and size within three smaller 10 × 10 cm quadrats haphazardly deployed on hard substrate within the larger quadrat. To complement the previous dataset, we monitored a fourth site within China Camp (Bullhead Flat; electronic supplementary material, appendix S2) at least every four months from December 2009 to May 2014. For this dataset, we quantified the number of oysters within 10 of 0.063 m^2 quadrats that we randomly distributed along a 30 m transect at 0.0 m MLLW. For each quadrat, we measured the longest shell length of the first 10 oysters encountered. If the quadrat did not contain at least 50% hard substrate, then the quadrat was shifted along the transect until this condition was met. We report only oyster size frequency data from Bullhead Flat because this was the longest time series available; however; size data were collected from the other sites, which exhibited similar patterns. Lastly, we measured oyster recruitment at Bullhead Flat, using 10.8 × 10.8 cm ceramic tiles that acted as settlement surfaces for recruits. We deployed the tiles facing downward on polyvinyl chloride (PVC) frames at 0.0 m MLLW. We recovered these tiles every three months between 2012 and 2013 and monthly in 2014 for a total of 16 sampling events and 89 tiles (three to six tiles per time point, mean = 5.6 tiles). After recovery, we counted recruits, using dissecting microscopes in the laboratory. For all oyster data, we report and plot abundances as counts m^{-2}.

(d) Statistics

We used extreme value analysis [43] to estimate the return time of discharge events greater than or equal to the event coincident with oyster mass mortality. Given a sufficiently long time series, a return time estimates the expected time between extremes. We used extreme value analysis because it accounts for the fact that the distribution of extreme events may have 'heavy tails' (decaying at a slower rate than expected) and is preferable to approaches that use error distributions (e.g. gamma, lognormal) that may underestimate the occurrence of extremes [44]. Because the available salinity data only span 9 years, we used Dayflow data from 1929 to 2014 (86 years) for analysis. We used a 'block maxima' approach to calculate the return times of maximum discharge over annual blocks. Autocorrelation plots indicated that annual maximum discharge was independent between successive years, meeting an assumption of this statistical approach. For this time series, we evaluated the fit of the data to generalized extreme value distributions (i.e. Gumbel, Fréchet, and Weibull), using confidence intervals from the profiled likelihood. We then estimated the return time for the observed 2011 maximum discharge (=6 190 $m^3 s^{-1}$). We evaluated the assumption of stationarity by regressing year and annual maximum discharge and found no evidence of a temporal trend ($F_{1,84} = 0.91$, $p = 0.34$). We conducted all analyses, using R [45] and the packages 'extRemes' and 'ggplot2'.

3. Results

(a) Physical drivers

An extreme delta discharge event began on 16 March 2011 and subsequently peaked on 26 March 2011 with a flow of 6 190 $m^3 s^{-1}$, as compared with the annual median discharge of 560 $m^3 s^{-1}$. In March 2011, three AR2s and 10 AR1s (last AR2 shown in figure 1*a*) were associated with 37.0% and 32.3% of the total precipitation measured at all stations for that month, respectively (figure 1*b*). In contrast, in January and February 2011, zero AR2s and 10 AR1s made landfall with little observed precipitation (electronic supplementary material, appendix S5). For the entire 2010–2011 winter season (November–March), AR2s were observed on 20 occasions (most arriving in early winter), in comparison with an average of 9.4 per winter from 1998 to 2011 [38]. Multi-decadal precipitation records indicate that water year 2011 was above average for total precipitation and March continued this trend, with 2011 ending as the ninth wettest year (out of 94 years) for the Northern Sierra 8 index (figure 1*c*). This pattern was consistent for the Central and Southern Sierra precipitation indices where 2011 was the fifth and seventh wettest year on record, respectively (electronic supplementary material, appendix S6). This extreme discharge event resulted in sustained low salinity at China

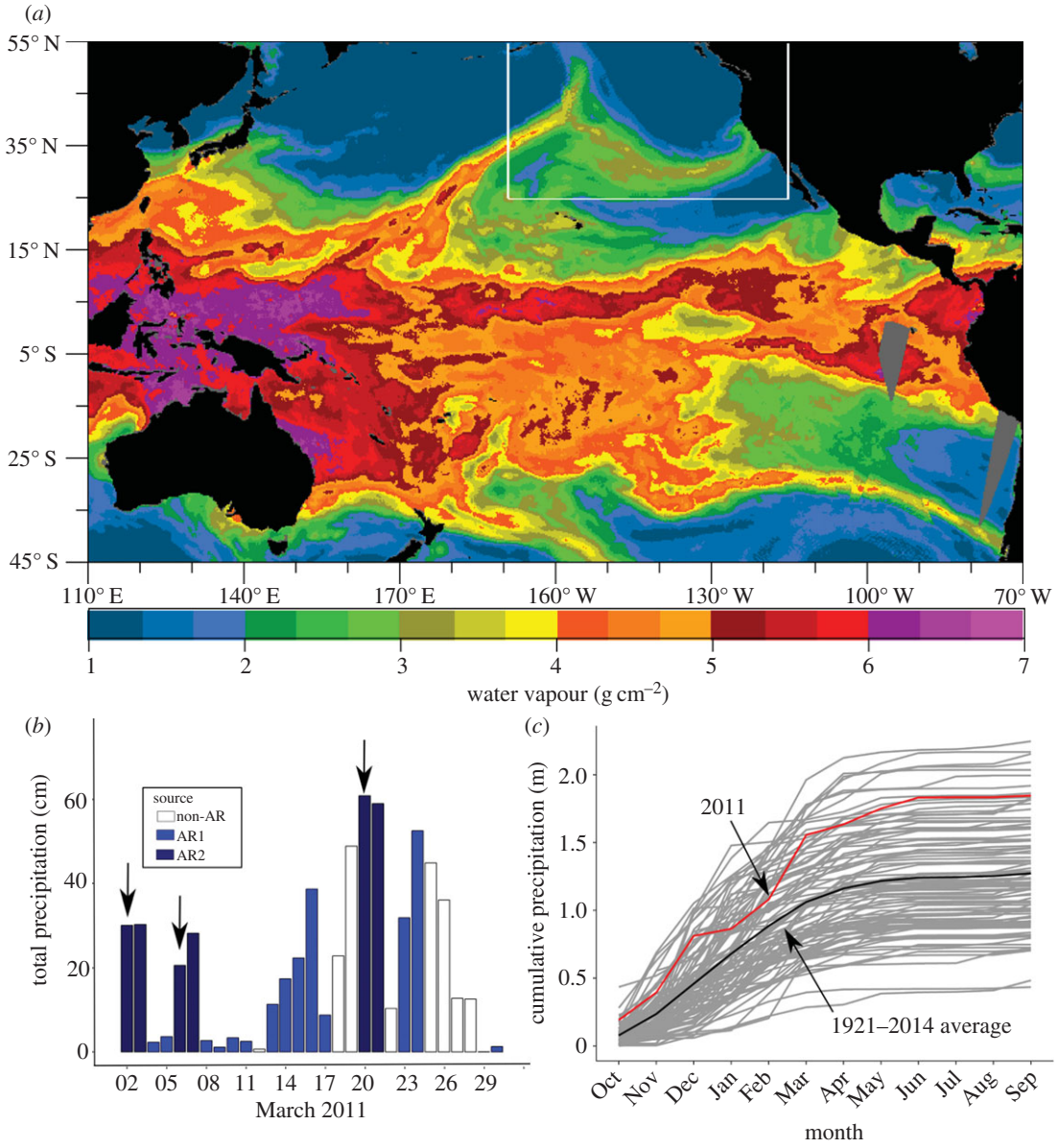

Figure 1. Atmospheric river (AR) occurrence and associated precipitation. (*a*) Atmospheric water vapour (ascending satellite pass) over the Pacific Ocean on 20 March 2011. Note the land falling AR on the western USA within the white box. (*b*) Total precipitation at 17 precipitation stations throughout the Sierra Nevada Mountain Range in March 2011. AR1s refer to ARs observed in either the morning or afternoon satellite pass. AR2s refer to ARs observed in both satellite passes. Precipitation is attributed to ARs if it fell on the date of landfall or the next day. Open bars refer to non-AR precipitation. Arrows refer to specific dates of AR2 landfall. (*c*) Monthly cumulative precipitation totals for the 'North Sierra 8' index from 1921 to 2014. Each line represents the cumulative precipitation trajectory for a single year. Red line is the year 2011 and the black line is the average cumulative precipitation for all years. Note the abrupt increase in precipitation in March 2011.

Camp that almost perfectly matched the critical salinity for oysters, which occurred during neap tides (electronic supplementary material, appendix S4 and S7). Salinity remained below 6.3 for eight continuous days, except for a brief excursion to 8.4 for 1 h 45 min (electronic supplementary material, appendix S7). Other potential stressors, such as air and water temperature, dissolved oxygen, and pH were well within oyster tolerance limits during this time period (electronic supplementary material, appendix S8).

Extreme value analysis indicated that the annual maximum discharge data were best fit by a Fréchet distribution (figure 4, shape parameter = 0.246, 95% CI = 0.0035–0.65). This model estimated a 3 year return time for a discharge of 6 126 $m^3 s^{-1}$ (95% CI = 4 961–7 291 $m^3 s^{-1}$), which closely approximates the discharge in 2011 that resulted in oyster mass mortality.

(b) Biological monitoring

Immediately prior to the extreme low salinity event, mean oyster counts ranged between 918 and 2 000 m^{-2} across sites. However, between sampling events in January and April 2011, oyster populations exhibited declines of 90%, 84%, 94%, and 90% at Bullhead Flat, Rat Rock, Village North, and Weber Point, respectively (figure 2*c*). During surveys in April 2011, we observed decomposing oyster tissue and gaping shells at all sites, indicative of recent mortality. By July 2011 at the same sites, oyster populations were even further reduced with 100%, 97%, 99%, and 99% mortality, respectively. In the following years, oyster abundance remained effectively zero at Bullhead Flat until November 2013 when oyster counts exceeded 1 600 oysters m^{-2} (figure 2*c*). Size frequency distributions prior to the 2011 event revealed a large spread in oyster sizes, suggesting multiple recruitment classes and

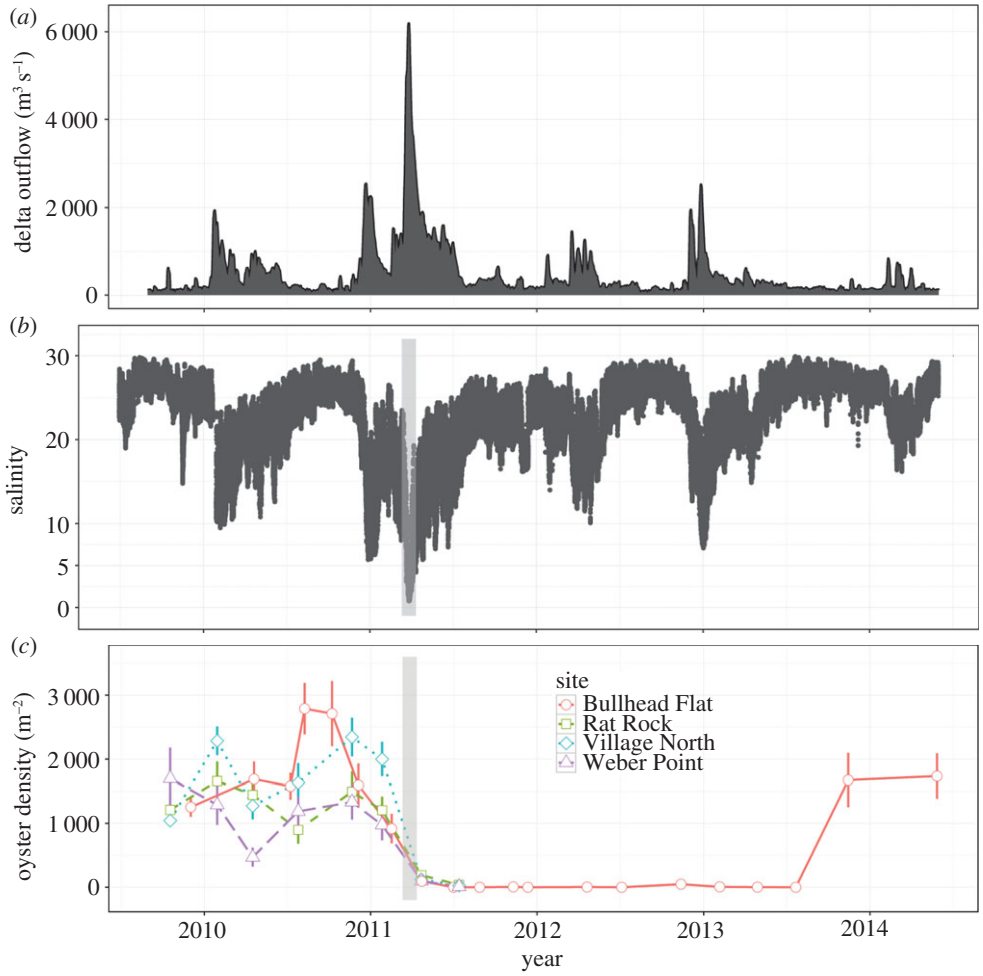

Figure 2. Time series of (*a*) delta outflow, (*b*) salinity measured at China Camp State Park, and (*c*) oyster density (mean ± standard error (s.e.)) at four sites within China Camp. Data from Rat Rock, Village North, and Weber Point were collected from October 2009 to July 2011. Bullhead Flat data were collected from December 2009 to May 2014. Shaded regions in (*b*) and (*c*) refer to the extreme discharge event and are plotted in electronic supplementary material, appendix S7 for a closer inspection of the salinity time series and tidal height.

survival of larger and presumably older individuals (figure 3). However, in 2012, the few oysters recorded alive were less than 30 mm in size, suggesting recent recruitment to the population (figure 3). The numerical recovery of oysters was coincident with recruitment beginning in July 2013, followed by substantial oyster recruitment in the summer of 2014 (electronic supplementary material, appendix S9).

4. Discussion

Climate change is expected to increase the frequency and severity of extreme events [1,2], with theory predicting that extreme precipitation events should intensify because of increased evaporation and greater atmospheric water-holding capacity [46]. However, the biological impacts of precipitation extremes are difficult to quantify because of the unpredictable nature of such events. ARs have emerged as a key process that contributes to precipitation extremes [13,14], but the biological impacts of these broad-scale features have not been described. Here, we document the occurrence of ARs with the mass mortality of wild oysters in northern San Francisco Bay. In March 2011, ARs contributed to extreme precipitation, coincident with high freshwater flows through the delta, resulting in sustained low salinities at China Camp (figures 1 and 2). Correlated with this extreme low salinity event, oyster abundance at northern San Francisco Bay sites declined by 97–100% (figure 2). Time-series data revealed that the salinity exposure almost perfectly matched the lower limit of oyster salinity tolerance (figure 2; [42]). In contrast, air and water temperatures, dissolved oxygen, and pH values remained well within known tolerance limits (electronic supplementary material, appendix S4 and S8). While this appears to be strong evidence for the role of ARs in contributing to the MME of wild oysters, we also note that these observations are correlative in nature. Further documentation of AR occurrence with discharge events is needed to validate the role of these features in driving environmental extremes and their impacts on biota.

Wild native oysters have experienced significant population declines over the last century and are therefore the focus of restoration and conservation efforts throughout the USA [49]. For Olympia oysters, recruitment is sporadic and in addition to eutrophication and substrate limitation, poor and variable recruitment is a contributing factor in the failed recovery of this species [50–52]. Extreme events may magnify the effects of poor recruitment, given that environmental extremes are projected to increase in frequency and intensity [2]. The northern San Francisco Bay population of oysters at China Camp represents the most abundant stock of Olympia oysters in San Francisco Bay (possibly throughout the species range; electronic supplementary material,

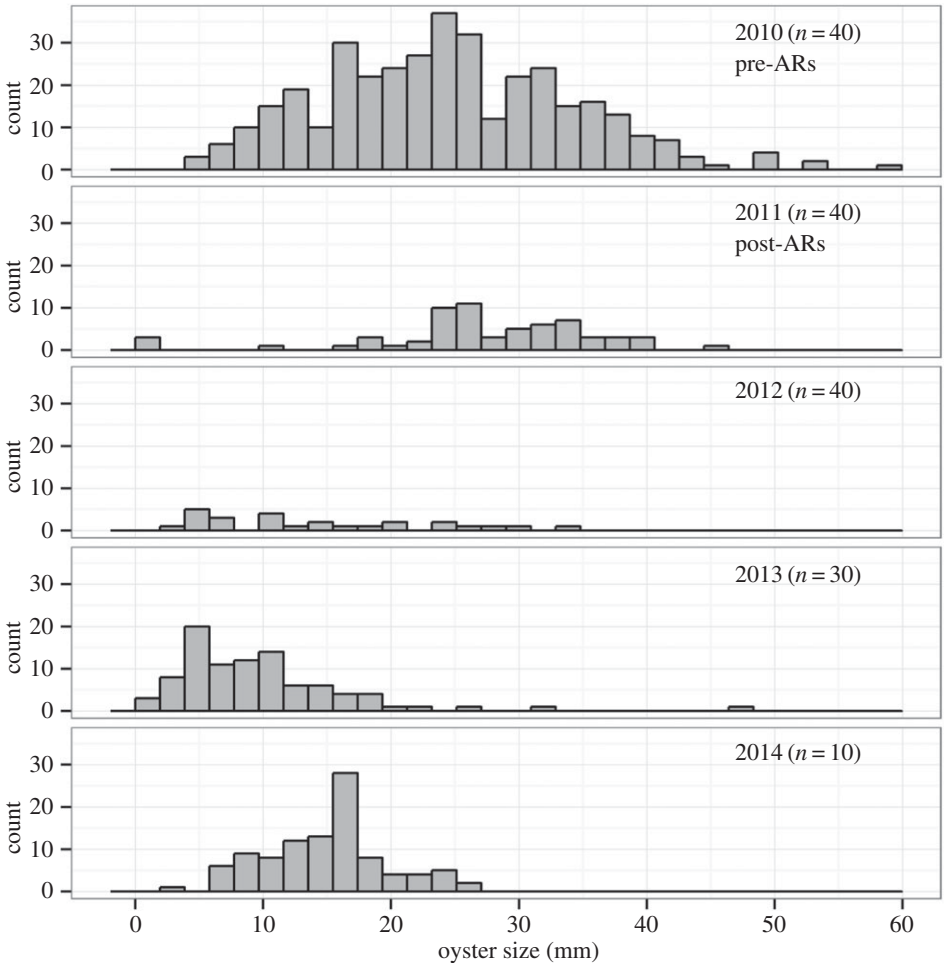

Figure 3. The impact of the low salinity event on oyster size frequency distributions at Bullhead Flat, China Camp. Size frequency data are binned by sample year from 1 March to 28 February, which separates the oyster data before and after the low salinity event. The low salinity event resulted in near 100% mortality of the population, but a small number of oysters were measured later in 2011. 2010 and 2011 had greater sampling than other years, so we randomly excluded a small number of sampling events to standardize sampling effort in the years before and after the low salinity event (2 and 1 sampling events excluded from 2010 and 2011, respectively). Sample size = number of quadrats.

appendix S1), and an MME of this population may have significantly reduced a source of oyster recruits to other parts of San Francisco Bay. Oysters appeared to have numerically recovered to pre-disturbance levels by November 2013, most likely rescued by other oyster populations within the estuary (e.g. South San Francisco Bay). However, they have yet to reach the broad size distribution of the population prior to the event (figure 3), suggesting that the reproductive potential of this population has yet to recover given that oyster reproductive output scales with age and size [53]. On the one hand, a 3 year return time for extreme low salinity events in northern San Francisco Bay initially suggests that this region may be suboptimal habitat for oysters, potentially acting as a population sink. However, Olympia oysters from San Francisco Bay are capable of first reproduction at four to eight months of age [54,55] and if able to persist, this population may act as a large source of recruits to other sites within the estuary. The potential significance of this population is compounded by evidence indicating that the region may contain oyster abundances much greater than typically found in other estuaries (electronic supplementary material, appendix S1; [33,34]). Climate change may alter these potential source–sink dynamics if flood events and extreme low salinities become more common, as is predicted by multi-model projections [6].

The proximate mechanism of this oyster MME was most likely the prolonged exposure to low salinity conditions. Oysters are osmoconformers (i.e. internal osmolality matches ambient conditions) and will first respond to low salinity conditions by sealing their mantle cavities from the external environment [56]. Prolonged valve closure is accompanied by metabolic depression and a switch to anaerobic metabolism [57]. However, this capacity is time limited by organismal tolerance of asphyxia and metabolic waste products [57]. Therefore, oysters are capable of tolerating short-term low salinity fluctuations but not prolonged low salinity extremes, such as the event recorded in March 2011. Oyster mortality from large-scale physical features (e.g. tropical cyclones) has been documented for wild eastern oysters (*C. virginica*), a species that appears to have greater tolerance to low salinity than Olympia oysters [58,59]. For example, Munroe *et al.* [58] observed that more than 20 days of salinity less than 7 was required for eastern oyster mortality of 55%. In contrast, Olympia oysters are only able to tolerate 8 days of salinities less than 6.3 [42]. This greater tolerance for low salinity by eastern oysters may have arisen due to selection, perhaps because cyclones and precipitation-driven salinity extremes are prominent recurring features of the western Atlantic Ocean. In contrast, eastern Pacific Ocean cyclone landfall in the USA is rare [60], and low salinity extremes

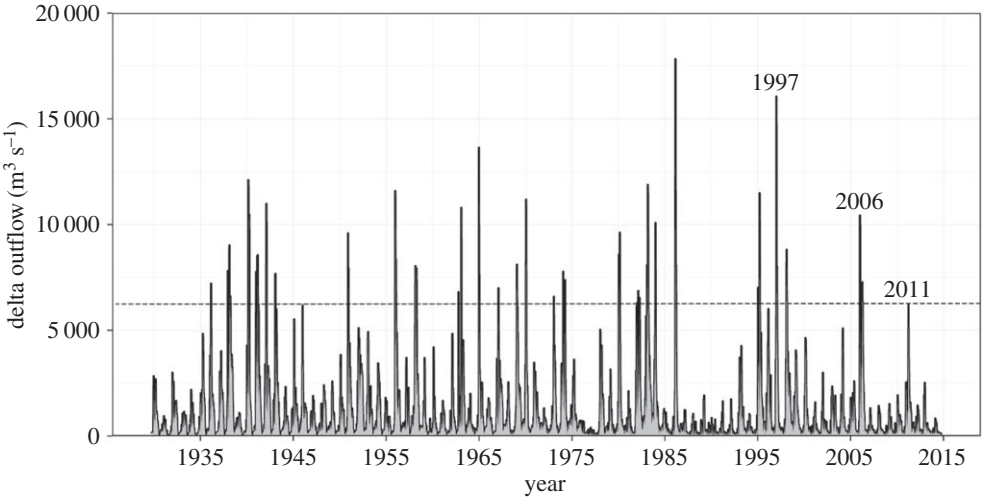

Figure 4. Time series of daily delta outflow (DayFlow) from 1929 to 2014. The dotted line marks the 2011 delta outflow that was coincident with oyster mass mortality. The 2006 extreme discharge event was caused by an AR that made landfall on 29–31 December 2005 [47] with delta outflow peaking on 3 January 2006. This discharge most likely caused salinity at China Camp to exceed lethal oyster limits as in 2011. The 1997 discharge event was driven by a Pacific cyclone and an accompanying AR that made landfall in California from 31 December 1996 to 1 January 1997 [48] with delta outflow peaking on 3 January 1997.

are less frequent and of relatively short duration [42]. These high salinity regimes may have resulted in little selection for prolonged low salinity tolerance, when compared with oysters within the genus *Crassostrea*. San Francisco Bay may be the exception for Olympia oysters, largely because of the vast watershed that the estuary drains. In response, oysters from northern San Francisco Bay appear to be locally adapted to modest exposures of low salinity [54], but relatively intolerant of prolonged and extreme low salinity as seen here. Understanding the capacity for these populations to adapt to changing environmental conditions represents a key challenge for biologists attempting to forecast species responses to climate change.

ARs have emerged as a key process that can drive extreme precipitation and subsequent flooding across the globe. On the west coast of the USA, extreme precipitation events appear to be largely driven by ARs [13,19] that are expected to intensify in response to greenhouse gas emissions [21,22]. Notably, the low salinity event in March 2011 occurred within the context of an already wet year, which was associated with a high frequency of winter AR occurrence. Evidence suggests that the ARs during the winter 2010–2011 were slightly weaker than the average during 1998–2011 [38]. Instead, it appears that the anomalously high frequency of winter AR occurrence led to heavy cumulative precipitation, which was correlated with large-scale atmospheric conditions (i.e. the Arctic Oscillation and the Pacific–North American teleconnection pattern; [38]). The wet conditions of early winter 2010–2011 likely created highly saturated soils, increasing the discharge potential of AR-associated precipitation later in March 2011 [12]. Historically, ARs have been correlated with extreme delta discharge events that surpassed the level seen in March 2011. In early January of 1997 and 2006, ARs [47,48] were associated with peak delta discharges over 16 000 $m^3 s^{-1}$ and 10 000 $m^3 s^{-1}$, respectively (figure 4). Although we lack quantitative oyster data from 1997 to 2006, high relative abundance at China Camp was recorded in 2003 [61]. By November 2006, China Camp oyster presence/absence surveys revealed no living oysters and many shell remains indicative of recent mortality [62], possibly a result of the AR-driven extreme freshwater discharge in January 2006. During that time, we also observed widespread mortalities of sessile invertebrates throughout much of San Francisco Bay [63]. Although the ecological impacts of ARs are difficult to measure because of their unpredictable landfall, coastal ecosystems such as estuaries may be 'hotspots' for examining such impacts because their watersheds collect and concentrate AR precipitation across a wide geographical area (i.e. the watershed).

5. Conclusion

Extreme events are predicted to be more prevalent under climate change. However, understanding the ecological consequences of such extremes is hindered by their unpredictable nature. We highlight a new mechanism by which precipitation extremes appear to affect a sensitive species, contributing to the near 100% mass mortality of wild oysters in northern San Francisco Bay. We estimate that ARs were associated with 69.3% of the precipitation during the run up to an extreme discharge event into the estuary. This discharge resulted in a protracted low salinity event that exceeded the critical low salinity tolerance for wild Olympia oysters. Several years after the MME, although oysters recovered numerically, their reproductive output has likely not reached pre-disturbance levels because of their small size. This is significant because this population may be the most dense and abundant stock throughout the species range. In the long term, the persistence of oysters in northern San Francisco Bay will likely depend on dispersal and rescue effects by other oyster populations within the estuary. However, climate models suggest that this region will experience increased frequency and intensity of precipitation extremes [6,36,37], which may affect the persistence of this recovering population.

For the MME described here, we used a substantial amount of publicly available data. The need for time-series data to describe causal mechanisms of MMEs highlights the importance of environmental monitoring networks and publicly available data in understanding the effects of global environmental change. However, physical monitoring is most powerful when accompanied by standardized sampling of biological communities. Long-term monitoring networks

clearly have a crucial function in describing the impacts of extremes, MMEs, and the broad-scale impacts of global change on natural communities [64]. Investigating how extremes, in addition to trends, affect natural ecosystems represents an important step in developing an understanding of how species will cope with ongoing and future environmental change.

Ethics. All research adhered to local and state guidelines. Field data were collected under CDFW permits SC-4765/6054/10238.

Data accessibility. Discharge data are available from the California Department of Water Resources (www.water.ca.gov/dayflow/). SSMIS data are produced by Remote Sensing Systems and sponsored by the NASA Earth Science MEaSUREs Programme. Data are available from Remote Sensing Systems (www.remss.com). Precipitation data are available from the California Data Exchange Center (http://cdec.water.ca.gov/snow_rain.html/). Sea surface level data are available from NOAA (https://tidesandcurrents.noaa.gov/). Water quality data are available from NERRS (http://cdmo.baruch.sc.edu/). Biological data are available at Dryad (http://dx.doi.org/10.5061/dryad.p0r3v).

Authors' contributions. All contributors designed the study, collected field data, and wrote the paper. B.S.C. conducted statistical analyses. All authors gave final approval for publication.

Competing interests. We have no competing interests.

Funding. Support was provided by: NERRS Collaborative Science (to B.S.C., A.L.C., A.D., M.C.F.; NOAA grant no. NA09NOS4190153), NERRS Graduate Research Fellowship (B.S.C.), Smithsonian Institution Postdoctoral Fellowships (B.S.C. and A.L.C.), CALFED Science Programme (A.L.C), and by an award under the Federal Coastal Zone Management Act, administered by the National Oceanic and Atmospheric Administration's Office for Coastal Management (to San Francisco State University).

Acknowledgements. We thank Lara Martin, Rachel Endicott, Caitlin Coleman-Hulbert, Chris Raleigh, Sarah Ferner, Rosa Schneider, Katie Nuessly, and Raman Paul for the collection of NERRS water quality data. We also thank Betsy Wells, Preston Malm, Karissa Willits, Sarah Covello, Jessica Couture, Linsey Haram, and Lisa Komoroske for assistance collecting oyster data. The D.M. Society provided valuable support during analysis and writing. We thank Jared Lewis for assistance with precipitation data and Paul Neiman for water vapour data. Discussions with Paul Neiman and Mike Dettinger regarding ARs greatly improved the manuscript. We finally thank Cathy Pfister and two anonymous reviewers for their constructive comments.

References

1. Easterling DR, Meehl GA, Parmesan C, Changnon SA, Karl TR, Mearns LO. 2000 Climate extremes: observations, modeling, and impacts. *Science* **289**, 2068–2074. (doi:10.1126/science.289.5487.2068)
2. Coumou D, Rahmstorf S. 2012 A decade of weather extremes. *Nat. Clim. Change* **2**, 491–496. (doi:10.1038/nclimate1452)
3. Luterbacher J, Dietrich D, Xoplaki E, Grosjean M, Wanner H. 2004 European seasonal and annual temperature variability, trends, and extremes since 1500. *Science* **303**, 1499–1503. (doi:10.1126/science.1093877)
4. Stott PA, Stone DA, Allen MR. 2004 Human contribution to the European heatwave of 2003. *Nature* **432**, 610–614. (doi:10.1038/nature03089)
5. Groisman PY, Knight RW, Easterling DR, Karl TR, Hegerl GC, Razuvaev VAN. 2005 Trends in intense precipitation in the climate record. *J. Clim.* **18**, 1326–1350. (doi:10.1175/JCLI3339.1)
6. Yoon J-H, Wang SYS, Gillies RR, Kravitz B, Hipps L, Rasch PJ. 2015 Increasing water cycle extremes in California and in relation to ENSO cycle under global warming. *Nat. Commun.* **6**. (doi:10.1038/ncomms9657)
7. Trenberth KE, Dai A, Rasmussen RM, Parsons DB. 2003 The changing character of precipitation. *Bull. Am. Meteorol. Soc.* **84**, 1205–1217. (doi:10.1175/BAMS-84-9-1205)
8. Smith MD. 2011 An ecological perspective on extreme climatic events: a synthetic definition and framework to guide future research. *J. Ecol.* **99**, 656–663. (doi:10.1111/j.1365-2745.2011.01798.x)
9. Coma R, Ribes M, Serrano E, Jimenez E, Salat J, Pascual J. 2009 Global warming-enhanced stratification and mass mortality events in the Mediterranean. *Proc. Natl Acad. Sci. USA* **106**, 6176–6181. (doi:10.1073/pnas.0805801106)
10. Wernberg T, Smale DA, Tuya F, Thomsen MS, Langlois TJ, de Bettignies T, Bennett S, Rousseaux CS. 2013 An extreme climatic event alters marine ecosystem structure in a global biodiversity hotspot. *Nat. Clim. Change* **3**, 78–82. (doi:10.1038/nclimate1627)
11. Helmuth B, Harley CDG, Halpin PM, O'Donnell M, Hofmann GE, Blanchette CA. 2002 Climate change and latitudinal patterns of intertidal thermal stress. *Science* **298**, 1015–1017. (doi:10.1126/science.1076814)
12. Ralph FM, Coleman T, Neiman PJ, Zamora RJ, Dettinger MD. 2013 Observed impacts of duration and seasonality of atmospheric-river landfalls on soil moisture and runoff in coastal Northern California. *J. Hydrometeorol.* **14**, 443–459. (doi:10.1175/JHM-D-12-076.1)
13. Ralph FM, Neiman PJ, Wick GA, Gutman SI, Dettinger MD, Cayan DR, White AB. 2006 Flooding on California's Russian River: role of atmospheric rivers. *Geophys. Res. Lett.* **33**. (doi:10.1029/2006GL026689)
14. Neiman PJ, Ralph FM, Wick GA, Lundquist JD, Dettinger MD. 2008 Meteorological characteristics and overland precipitation impacts of atmospheric rivers affecting the West Coast of North America based on eight years of SSM/I satellite observations. *J. Hydrometeorol.* **9**, 22–47. (doi:10.1175/2007JHM855.1)
15. Zhu Y, Newell RE. 1998 A proposed algorithm for moisture fluxes from atmospheric rivers. *Mon. Weather Rev.* **126**, 725–735. (doi:10.1175/1520-0493(1998)126<0725:APAFMF>2.0.CO;2)
16. Ralph FM, Neiman PJ, Wick GA. 2004 Satellite and CALJET aircraft observations of atmospheric rivers over the eastern north pacific ocean during the winter of 1997/98. *Mon. Weather Rev.* **132**, 1721–1745. (doi:10.1175/1520-0493(2004)132<1721:SACAOO>2.0.CO;2)
17. Knippertz P, Martin JE. 2005 Tropical plumes and extreme precipitation in subtropical and tropical West Africa. *Q. J. R. Meteorol. Soc.* **131**, 2337–2365. (doi:10.1256/qj.04.148)
18. Gimeno L, Nieto R, Vázquez M, Lavers DA. 2014 Atmospheric rivers: a mini-review. *Front. Earth Sci.* **2**. (doi:10.3389/feart.2014.00002)
19. Dettinger MD, Ralph FM, Das T, Neiman PJ, Cayan DR. 2011 Atmospheric rivers, floods and the water resources of California. *Water* **3**, 445–478. (doi:10.3390/w3020445)
20. Lavers DA, Allan RP, Wood EF, Villarini G, Brayshaw DJ, Wade AJ. 2011 Winter floods in Britain are connected to atmospheric rivers. *Geophys. Res. Lett.* **38**. (doi:10.1029/2011GL049783)
21. Dettinger M. 2011 Climate change, atmospheric rivers, and floods in California—a multimodel analysis of storm frequency and magnitude changes. *J. Am. Water Resourc. Assoc.* **47**, 514–523. (doi:10.1111/j.1752-1688.2011.00546.x)
22. Warner MD, Mass CF, Salathe EP. 2015 Changes in winter atmospheric rivers along the North American West Coast in CMIP5 climate models. *J. Hydrometeorol.* **16**, 118–128. (doi:10.1175/JHM-D-14-0080.1)
23. Reed DH, O'Grady JJ, Ballou JD, Frankham R. 2003 The frequency and severity of catastrophic die-offs in vertebrates. *Anim. Conserv.* **6**, 109–114. (doi:10.1017/S1367943003003147)
24. Lande R. 1993 Risks of population extinction from demographic and environmental stochasticity and random catastrophes. *Am. Nat.* **142**, 911–927. (doi:10.1086/285580)
25. Gilpin ME, Soulé ME. 1986 Minimum viable populations: processes of extinction. In *Conservation biology: the science of scarcity and diversity* (ed. ME Soulé), pp. 19–34. Sunderland, MA: Sinauer Associates.

26. Lessios HA. 2016 The great *Diadema antillarum* die-off: 30 years later. *Ann. Rev. Mar. Sci*. 8, 267–283. (doi:10.1146/annurev-marine-122414-033857)
27. Fey SB, Siepielski AM, Nussle S, Cervantes-Yoshida K, Hwan JL, Huber ER, Fey MJ, Catenazzi A, Carlson SM. 2015 Recent shifts in the occurrence, cause, and magnitude of animal mass mortality events. *Proc. Natl Acad. Sci. USA* **112**, 1083–1088. (doi:10.1073/pnas.1414894112)
28. Kimbro DL, Grosholz ED. 2006 Disturbance influences oyster community richness and evenness, but not diversity. *Ecology* **87**, 2378–2388. (doi:10.1890/0012-9658(2006)87[2378:DIOCRA]2.0.CO;2)
29. Coen LD, Brumbaugh RD, Bushek D, Grizzle R, Luckenbach MW, Posey MH, Powers SP, Tolley SG. 2007 Ecosystem services related to oyster restoration. *Mar. Ecol. Prog. Ser*. **341**, 303–307. (doi:10.3354/meps341303)
30. Zu Ermgassen PSE *et al.* 2012 Historical ecology with real numbers: past and present extent and biomass of an imperilled estuarine habitat. *Proc. R. Soc. B* **279**, 3393–3400. (doi:10.1098/rspb.2012.0313)
31. Beck MW *et al.* 2011 Oyster reefs at risk and recommendations for conservation, restoration, and management. *Bioscience* **61**, 107–116. (doi:10.1525/bio.2011.61.2.5)
32. Kirby MX. 2004 Fishing down the coast: historical expansion and collapse of oyster fisheries along continental margins. *Proc. Natl Acad. Sci. USA* **101**, 13 096–13 099. (doi:10.1073/pnas.0405150101)
33. Polson MP, Zacherl DC. 2009 Geographic distribution and intertidal population status for the Olympia oyster, *Ostrea lurida* Carpenter 1864, from Alaska to Baja. *J. Shellfish Res.* **28**, 69–77. (doi:10.2983/035.028.0113)
34. Cheng BS, Grosholz ED. 2016 Environmental stress mediates trophic cascade strength and resistance to invasion. *Ecosphere* **7**. (doi:10.1002/ecs2.1247)
35. Conomos TJ, Smith RE, Gartner JW. 1985 Environmental setting of San Francisco Bay. *Hydrobiologia* **129**, 1–12. (doi:10.1007/BF00048684)
36. Cloern JE *et al.* 2011 Projected evolution of California's San Francisco Bay-Delta-river system in a century of climate change. *PLoS ONE* **6**, e24465. (doi:10.1371/journal.pone.0024465)
37. Min S-K., Zhang X, Zwiers FW, Hegerl GC. 2011 Human contribution to more-intense precipitation extremes. *Nature* **470**, 378–381. (doi:10.1038/nature09763)
38. Guan B, Molotch NP, Waliser DE, Fetzer EJ, Neiman PJ. 2013 The 2010/2011 snow season in California's Sierra Nevada: role of atmospheric rivers and modes of large-scale variability. *Water Resour. Res.* **49**, 6731–6743. (doi:10.1002/wrcr.20537)
39. Neiman PJ, Schick LJ, Ralph FM, Hughes M, Wick GA. 2011 Flooding in Western Washington: the connection to atmospheric rivers. *J. Hydrometeorol.* **12**, 1337–1358. (doi:10.1175/2011JHM1358.1)
40. Warner MD, Mass CF, Salathe EP. 2012 Wintertime extreme precipitation events along the Pacific Northwest coast: climatology and synoptic evolution. *Mon. Weather Rev.* **140**, 2021–2043. (doi:10.1175/MWR-D-11-00197.1)
41. Monismith SG, Kimmerer W, Burau JR, Stacey MT. 2002 Structure and flow-induced variability of the subtidal salinity field in northern San Francisco Bay. *J. Phys. Oceanogr*. **32**, 3003–3019. (doi:10.1175/1520-0485(2002)032<3003:SAFIVO>2.0.CO;2)
42. Cheng BS *et al.* 2015 Testing local and global stressor impacts on a coastal foundation species using an ecologically realistic framework. *Glob. Change Biol.* **21**, 2488–2499. (doi:10.1111/gcb.12895)
43. Coles S. 2001 *An introduction to statistical modeling of extreme values*. London, UK: Springer.
44. Katz RW, Brush GS, Parlange MB. 2005 Statistics of extremes: modeling ecological disturbances. *Ecology* **86**, 1124–1134. (doi:10.1890/04-0606)
45. R Core Team. 2016 *R: a language and environment for statistical computing*. Vienna, Austria: R Foundation for Statistical Computing.
46. Trenberth KE. 1999 Conceptual framework for changes of extremes of the hydrological cycle with climate change. *Clim. Change* **42**, 327–339. (doi:10.1023/A:1005488920935)
47. Smith BL, Yuter SE, Neiman PJ, Kingsmill DE. 2010 Water vapor fluxes and orographic precipitation over northern California associated with a landfalling atmospheric river. *Mon. Weather Rev*. **138**, 74–100. (doi:10.1175/2009MWR2939.1)
48. Galewsky J, Sobel A. 2005 Moist dynamics and orographic precipitation in northern and central California during the new year's flood of 1997. *Mon. Weather Rev.* **133**, 1594–1612. (doi:10.1175/MWR2943.1)
49. McGraw KA. 2009 The Olympia oyster, *Ostrea lurida* Carpenter 1864 along the West coast of North America. *J. Shellfish Res*. **28**, 5–10. (doi:10.2983/035.028.0110)
50. Seale EM, Zacherl DC. 2009 Seasonal settlement of Olympia oyster larvae, *Ostrea lurida* Carpenter 1864 and its relationship to seawater temperature in two southern California estuaries. *J. Shellfish Res*. **28**, 113–120. (doi:10.2983/035.028.0103)
51. Brumbaugh RD, Coen LD. 2009 Contemporary approaches for small-scale oyster reef restoration to address substrate *versus* recruitment limitation: a review and comments relevant for the Olympia Oyster, *Ostrea lurida* Carpenter 1864. *J. Shellfish Res*. **28**, 147–161. (doi:10.2983/035.028.0105)
52. Trimble AC, Ruesink JL, Dumbauld BR. 2009 Factors preventing the recovery of a historically overexploited shellfish species, *Ostrea lurida*, Carpenter 1864. *J. Shellfish Res*. **28**, 97–106. (doi:10.2983/035.028.0116)
53. Kang S-G, Choi K-S, Bulgakov AA, Kim Y, Kim S-Y. 2003 Enzyme-linked immunosorbent assay (ELISA) used in quantification of reproductive output in the pacific oyster, *Crassostrea gigas*, in Korea. *J. Exp. Mar. Biol. Ecol*. **282**, 1–21. (doi:10.1016/S0022-0981(02)00444-6)
54. Bible JM, Sanford E. 2016 Local adaptation in an estuarine foundation species: implications for restoration. *Biol. Conserv.* **193**, 95–102. (doi:10.1016/j.biocon.2015.11.015)
55. Moore JD, Marshman BC, Obernolte R, Abbott R. in press Sexual development and symbionts of native Olympia oysters *Ostrea lurida* naturally settled on cultch deployed in San Francisco Bay, California. *Calif. Fish Game*.
56. Berger VJ, Kharazova AD. 1997 Mechanisms of salinity adaptations in marine molluscs. *Hydrobiologia* **355**, 115–126. (doi:10.1023/A:1003023322263)
57. De Zwaan A, Wijsman TCM. 1976 Anaerobic metabolism in Bivalvia (Mollusca)—characteristics of anaerobic metabolism. *Comp. Biochem. Physiol. B Biochem. Mol. Biol.* **54**, 313–323. (doi:10.1016/0305-0491(76)90247-9)
58. Munroe D, Tabatabai A, Burt I, Bushek D, Powell EN, Wilkin J. 2013 Oyster mortality in Delaware Bay: impacts and recovery from Hurricane Irene and Tropical Storm Lee. *Estuar. Coast. Shelf Sci.* **135**, 209–219. (doi:10.1016/j.ecss.2013.10.011)
59. Livingston RJ, Howell RL, Niu XF, Lewis FG, Woodsum GC. 1999 Recovery of oyster reefs (*Crassostrea virginica*) in a gulf estuary following disturbance by two hurricanes. *Bull. Mar. Sci.* **64**, 465–483.
60. Chenoweth M, Landsea C. 2004 The San Diego Hurricane of 2 October 1858. *Bull. Am. Meteorol. Soc.* **85**, 1689–1697. (doi:10.1175/BAMS-85-11-1689)
61. Harris HE. 2004 *Distribution and limiting factors of* Ostrea conchaphila *in San Francisco Bay*. San Francisco, CA: San Francisco State University.
62. Grosholz E, Moore J, Zabin C, Attoe S, Obernolte R. 2007 Planning for native oyster restoration in San Francisco Bay. Final Report to California Coastal Conservancy Agreement no 05-134.
63. Chang AL. 2009 An urban estuary in a changing world: diversity, invasions, and climate change in San Francisco Bay. University of California, Davis.
64. Anderson-Teixeira KJ *et al.* 2015 CTFS-ForestGEO: a worldwide network monitoring forests in an era of global change. *Glob. Change Biol.* **21**, 528–549. (doi:10.1111/gcb.12712)